HiSST: 3rd International Conference on
High-Speed Vehicle Science Technology
14 -19 April 2024, Busan, Korea

Operational Characteristics of a Liquid-Fueled Regenerative Dual-mode Combustor Model with Small Inlet Flowpath Height

Inyoung Yang[1], Sanghun Lee[2], Kyungjae Lee[3], Yangji Lee[4]

Abstract

Experimental research was performed for a liquid-fueled regenerative supersonic combustor model. The model features a small inlet flowpath height of 20 mm, which is typical in many scaled experimental research models. Flow speed at model inlet was Mach 2, total pressure was 800 kPa(abs), and total temperature was 1,290 K which are corresponding to Mach 5 flight condition. The test campaign was done at various fuel flow rate with fixed model geometry and fixed inlet flow condition. Fuel was heated by regenerative heat exchangers before supplied to the injector. The fuel injection condition was varied with various test conditions, in the range of 1.0-2.1 MPa(abs) and 483-493 °C. Transition from scramjet mode to ramjet mode was observed in the model at relatively low fuel equivalence ratio of 0.19. Mode transition at such a low fuel equivalence is addressed to the small inlet flowpath height, by which the effect of boundary layer becomes dominant in the model. The transition was detectable by the wall static pressure distribution, as well as by the direct optical observation of the flame.

Keywords: *Supersonic combustion, Liquid hydrocarbon fuel, Regenerative heat exchanger, Mode transition, Turbine-based combined cycle*

Nomenclature

N/A

1. Introduction

Scramjet engine or dual-mode scramjet engine has been considered as a propulsion system for hypersonic flight. It is especially regarded as an "efficient" propulsion system thanks to its air-breathing nature. Hypersonic flight by this type of engine have been realized using many types of fuels including hydrogen, gaseous hydrocarbon or liquid hydrocarbon, but liquid hydrocarbon may be the only possible fuel for practical, civilian use of this type of engine.

The authors also have been studied this engine using all those types of fuels, and concluded that the usage of liquid hydrocarbon should be accompanied with fuel heating. The problems of atomization, vaporization and slow ignition should be resolved partly by using fuel heating. One of the simplest way to realize fuel heating at ground test is regeneration, therefore, the authors are adopting the regeneration in their combustor test models.

In the authors' previous research, a combustor model with the inlet height of 32 mm had been used and tested in many sub-combustor level component configurations [1-3]. The test result revealed that, although the test campaign covered the fuel equivalence ratios from 0.05 to 0.33, mode transition to ram mode was never realized when only kerosene was used as fuel, i.e. with no auxiliary fuel such as hydrogen. Therefore, all successful operations with only kerosene fuel were actually in scramjet mode.

[1] *Korea Aerospace Research Intitute, Gwahak-ro 169-84, Yuseong-gu, Daejeon, South Korea, iyyang@kari.re.kr*
[2] *Korea Aerospace Research Intitute, Gwahak-ro 169-84, Yuseong-gu, Daejeon, South Korea, hunsh@kari.re.kr*
[3] *Korea Aerospace Research Intitute, Gwahak-ro 169-84, Yuseong-gu, Daejeon, South Korea, lucia01@kari.re.kr*
[4] *Korea Aerospace Research Intitute, Gwahak-ro 169-84, Yuseong-gu, Daejeon, South Korea, mars336@kari.re.kr*

The authors assumed that some design modification is required to realize the mode transition, including flow path height reduction.

Present research is aiming to develop a small-scale, ground test model for a turbine-based combined cycle engine [4]. The test model will be consisting of an integrated intake, a combustor model, and a gas turbine model. They are planned to be developed independently first, and integrated and tested in a freejet facility. And because the freejet facility's nozzle size is limited, the present combustor model height is restricted to be 20 mm. Therefore, in this research, operational characteristics of the combustor model with 20 mm inlet height were investigated using experimental methods. Although not only the flow path height was changed compared to the previous model, the effect of geometry change including the flow path height is expected be addressed by comparing the test results for those combustor models.

2. Test model and test facility

2.1. Test model

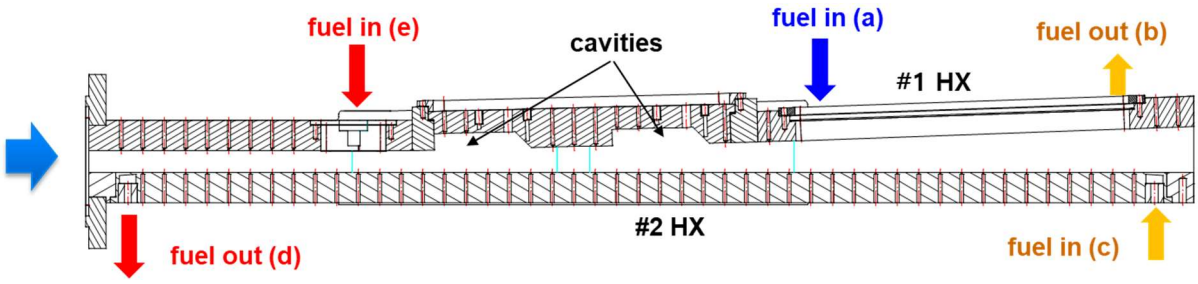

Fig. 1 Dual-mode combustor test model

Fig. 1 shows the dual-mode combustor model used in this research. The flowpath is 20 mm high and 100 mm wide at the model inlet, with the aspect ratio of 5. The flowpath height is kept constant until 300 mm downstream of the model inlet, and starts to increase thereafter, and finally becomes 41.9 mm at the model outlet.

Fuel injector set is located at 250 mm downstream of the model inlet. The injector set consists of four circular injection holes, each of which has 1 mm of diameter. The holes are arranged in transverse direction to the main flow direction, with the spacing of 16 mm.

There are two cavities at the top side of the model located in tandem configuration. The upstream cavity starts at 70 mm downstream of the injector. Its depth is 15 mm, and length is 75 mm. There is a 45° aft-ramp at the end of the cavity. The downstream cavity starts after 75 mm of the upstream cavity aft-ramp, and has the same configuration with the upstream cavity. There are two electric spark igniters, each of which installed at the bottom of the respective cavity.

The #1 regenerative heat exchanger is located downstream of the cavities on the top side. The entire bottom wall is also a regenerative heat exchanger, designated as #2. The two heat exchangers are connected in serial, therefore the fuel flow circuit in Fig. 1 is (a) → (b) → (c) → (d) → (e). The cross-sectional view of the #1 heat exchanger is shown in Fig. 2. There are 15 fuel flow paths, each of which has 3 mm width and 1.33 mm height. The spacing between the fuel flow paths is 1 mm, and the thickness of the combustor wall between the fuel flow path and the combustion gas path is 2 mm. The #2 heat exchanger has the same fuel flow path configuration, except that the flow path in the middle is removed to install pressure measurement tabs. The length of the fuel flow path is 270 mm for the #1 heat exchanger and 935 mm for the #2.

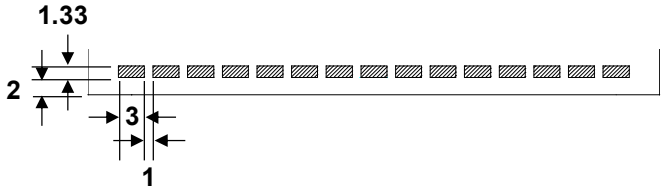

Fig. 2 Regenerative heat exchanger flow path configuration

Pressure tabs with 1 mm diameter are located along the center line of the model's top wall and bottom wall. But the #1 heat exchanger has no pressure tabs. Additionally, the pressure tabs on the isolator portion of the bottom wall were not used in this test campaign.

2.2. Direct-connected supersonic combustor test facility

Fig. 3 Direct-connected supersonic combustor test facility

The test facility used in this research is shown in Fig. 3. It is direct-connected type, and can provide a flow condition corresponding to that of Mach 5 flight condition at the combustor model inlet. Further details on the facility can be found in reference [5]. The detail flow condition is shown in table 1. The high-pressure air is provided by a continuous turbo-compressor. It is first heated by an electric air heater up to 600 K, and then enters to a vitiated air heater and heated up to the desired temperature. Make-up oxygen is provided to the vitiated air to maintain the oxygen concentration the same with that of fresh air. Fuel is supplied using a pump which can control the flow rate from the pump, regardless of the back pressure.

Table 1. Flow Condition

Speed	Total pressure	Total temp.	Static pressure	Static temp.	Air flow rate
Mach 2.0	800 kPa	1,290 K	95 kPa	710 K	0.95 kg/s

2.3. Test condition

Tests were performed with various fuel equivalence ratio values. Because the geometry of the test model and the air flow condition were kept unchanged, the only test variable of the test campaign is the fuel flow rate. The fuel flow rates and corresponding fuel equivalence ratios are shown in table 2.

Table 2. Test Conditions

Fuel flow rate (g/s)	8	12	16
Fuel equivalence ratio φ	0.12	0.19	0.25

3. Test results and discussion

3.1. Flame shape and overall behavior

Fig. 4. shows the flame images at various fuel equivalence ratio values. Fig. 4(a) is that at φ=0.12, and one can observe some "wavy" structure on the flame edge. Combined with the analyses on the wall static pressure distribution as discussed in sections 3.2 and 3.3, this wavy structure is found to be a characteristic feature of a scramjet mode flame. Also one can point out that the flame starts at the leading edge of the first cavity, and the first cavity is more filled with the flame compared to the second cavity. For the second cavity, the flame exists only around the shear layer.

Fig. 4(b) at φ=0.19 and at t=28 s shows that the cavities, especially the second cavity, are more filled with the flame compared to the Fig. 4(a). And the flame is stretched more in transversal direction. These are due to the larger fuel equivalence ratio. Except for these, the flame shape is not that much different from Fig. 4(a). The wavy structure on the flame edge is still found in the figure. Again, the flame is also in scramjet mode as is the previous case.

Fig. 4(c) is for the same φ with Fig. 4(b), but the figure was taken 6 seconds later than that. One can observe in Fig. 4(c) that the wavy structure disappeared. It can be also noted that the flame became shorter and more reddish compared with Fig. 4(b). This is because heat release became more concentrated around the cavities. With all these observations combined with the pressure analyses, one can assume that the flame mode transition from scramjet mode to ramjet mode occurred at some time between Fig. 4(b) and 4(c).

For a fixed fuel equivalence ratio, mode transition according to time may be attributed to the change in fuel injection condition according to time. Fuel injection condition, i.e. pressure and temperature, changes during the test because the fuel was heated by the regenerative heat exchanger. This fuel injection condition change is discussed in more detail in section 3.4.

Unfortunately, picture for the case of φ=0.25 was not taken. That case will be discussed later using wall static pressure data only.

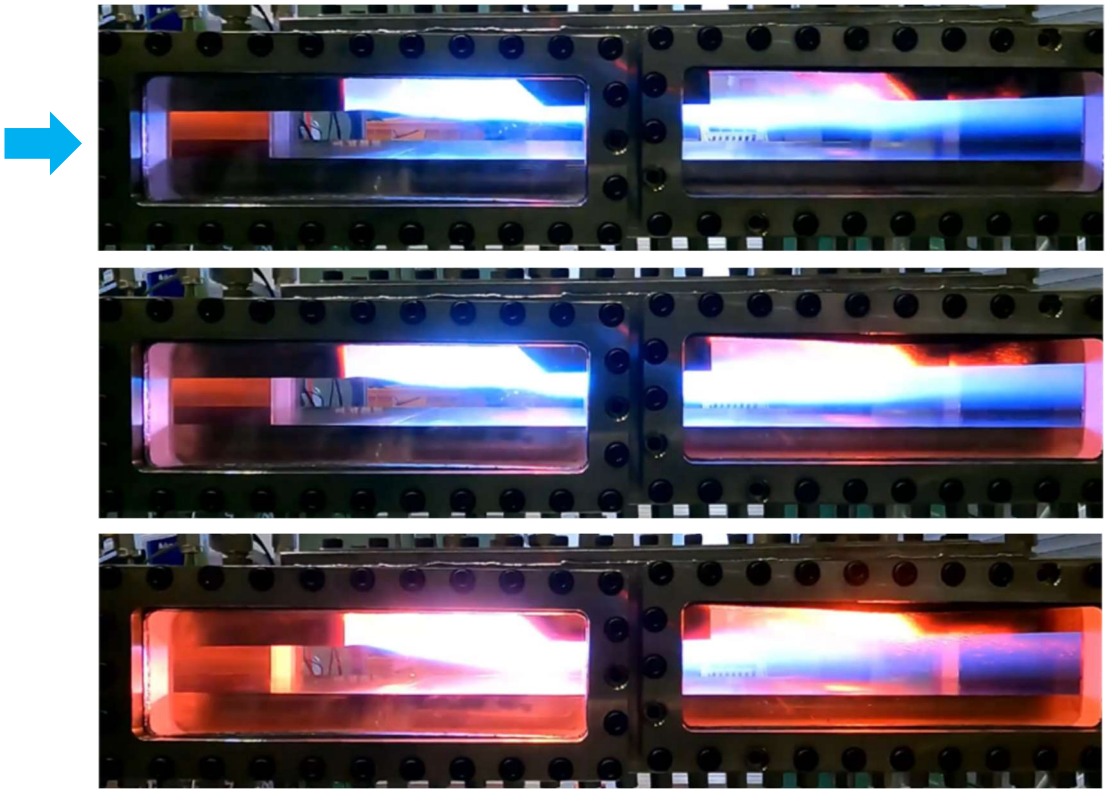

Fig. 4 Flame images (top: (a) φ=0.12, middle: (b) φ=0.19 (at t=28 s), bottom: (c) φ=0.19 (at t=34 s))

3.2. Time history of the wall static pressure

Fig. 5 is the time history of the combustor wall static pressure at various fuel equivalence ratio values. The pressures in the figure were measured at the locations of D14-D17 shown in Fig. 6, corresponding to the region on the bottom wall opposite to the first cavity. In Fig. 5(a) corresponding to φ=0.12, compared to Figs. 5(b) and 5(c), there is no abrupt change in pressure, indicating that there is no mode transition for this case. This was also confirmed by observing the flame video as discussed previously in section 3.1.

Regarding φ=0.19 case, as discussed later in section 3.4, the fuel supply valve was open before t=17 s and fuel temperature at the fuel injector location started to increase at t=18.7 s. The wall static pressures start to change at that time as in Fig. 5(b), and continue to change smoothly until t=28.4 s. And, one can find that the pressures increase abruptly at t=28.4 s. The pressures stay around 240-250 kPa(abs) during t=28.4-34.5 s. Therefore, it can be said that there is some abrupt change in the combustion flow field at t=28.4 s. Combined with the analyses on the flame video discussed in section 3.1, and on the spatial distribution of the wall static pressure discussed below, one can conclude that the change at t=28.4 s is actually flame mode transition.

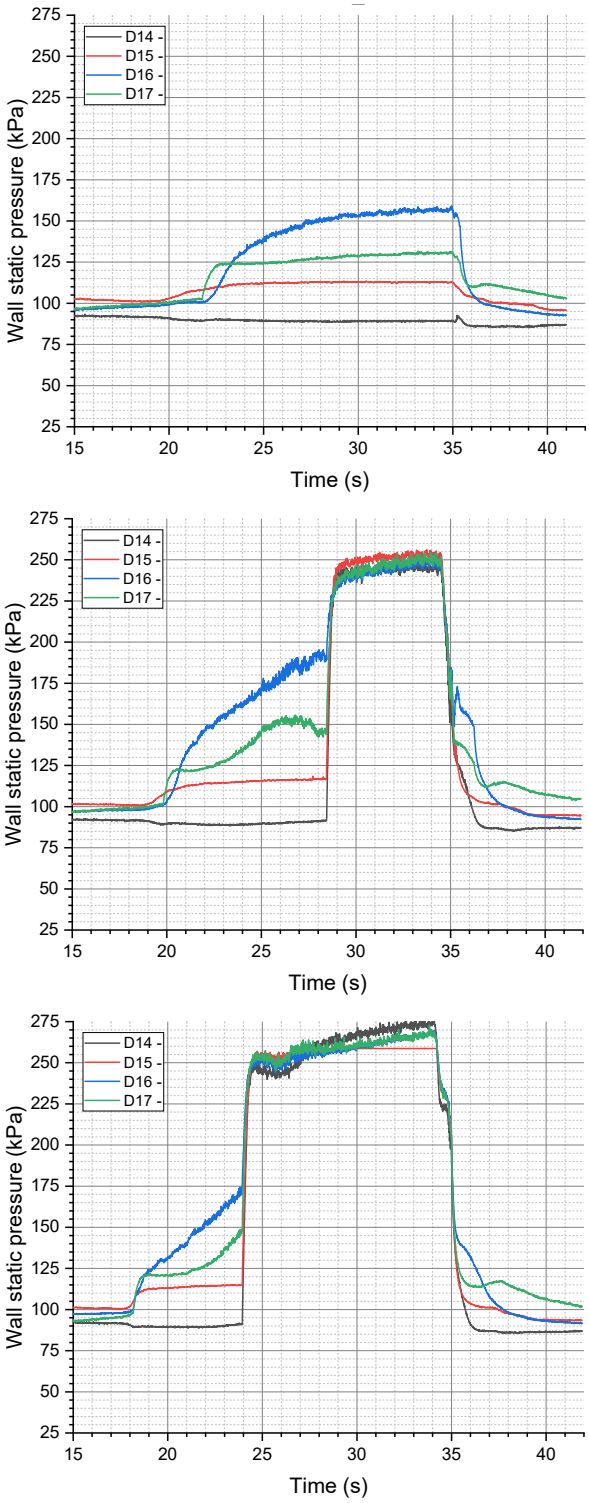

Fig. 5 Time history of the wall static pressure (top: (a) φ=0.12, middle: (b) φ=0.19, bottom: (c) φ=0.25 case)

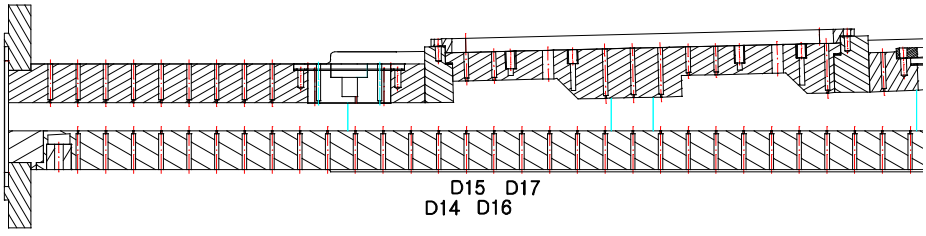

Fig. 6 pressure measurement locations

One more thing to note is that the pressures during the period of t=18.7-28.4 s show different transient behaviors according to their location. For an example, pressure at D15 increases in short period in t=19-21 s and remains nearly constant during most of the period. On the other hand, pressures at D16 and D17 show relatively gradual change during the entire period. This may indicate the difference in the cause of the pressure increase at difference locations. In other words, the pressure increase at D15 may be due to the shock generated by the fuel injection, while those at the other locations may be because of the heat release by combustion, which changes gradually in this study.

The gradual change of the combustion heat release may be attributed to the gradual change in fuel injection condition, as discussed later in section 3.4. In turn, the gradual change in fuel injection condition may be due to the large thermal inertia of the regenerative heat exchanger. In that case, the gradual change of the combustion heat release may be regarded as one of the characteristics of a regenerative combustor. But at the same time, it should be noted that during the ram mode phase, t=29-34.5 s in Fig. 5(b), the pressures remain relatively constant while the fuel condition still changes, even though the change is not as large as in the scram mode phase.

Fig. 5(c) for φ=0.25 shows similar behavior with that for φ=0.19. The greatest difference may be that the mode transition occurs much earlier than the former case.

3.3. Spatial distribution of the wall static pressure

As shown above in Fig. 5, there is some time period at the end of the combustion during which the wall static pressures remain relatively constant. Those pressures are regarded to be "steady" in this period. One-second or half-second in this steady period was selected and the average of each measurement location was taken to build the average spatial distribution along the combustor model, as shown in Fig. 7.

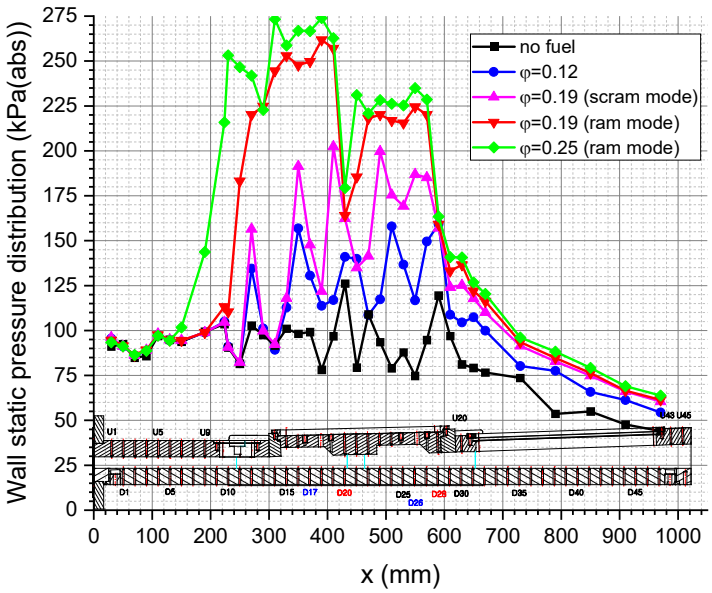

Fig. 7 Wall static pressure distribution

The distribution also confirms the mode transition discussed above. For φ=0.12 case, the distribution in the location range of x<600 mm shows clear shock structure of the flow and it increases in overall in that range. For "scram mode" case of φ=0.19, the shock structure becomes even clearer in the same location and also shows the same overall increase.

On the other hand, in "ram mode" case of φ=0.19, the pressure reaches maximum at x=390 mm where corresponds to the end of the upstream cavity, and decreases thereafter. Then, the pressure increases again after x=430 mm, reaching a second maximum at x=470 mm. There created a second plateau in the region of x=470-570 mm. This second maximum is attributed to the second cavity of the combustor model. In other words, this is a characteristic of a tandem-cavity combustor.

Also, for the same case, one can find that the pressure increases slightly at upstream of the fuel injector,

x=220 mm, which is again a typical characteristics of ramjet mode pressure distribution.

For the "ram mode" of the φ=0.25 case, the overall shape of the distribution is the same with that of the "ram mode" of the φ=0.19 case, but the pressure values become a little larger. One should also note that the starting point of the pressure increase in the isolator is x=150 mm, which is further upstream than that for φ=0.19 case. It is almost at the half of the isolator length even with this relatively low fuel equivalence ratio.

3.3.1. Comparison with calculation

Fig. 8 shows the wall static pressure distribution from test measurement as well as calculation. In both of Fig. 8(a) and 8(b), the calculation predicts a little higher pressures than the test. This may be because, in calculation, the reaction scheme is simplified as one-step global reaction, and also the fuel is assumed to be vaporized perfectly at the injector outlet. Faster reaction is assumed in the calculation than in the test by this simplification and assumption. And this faster reaction assumption sometimes yields huge difference in the flow when the combustion mode predicted differently as shown in Fig. 8(a) for φ=0.12 case. In that case, the wall static pressure distributions from test and calculation show totally difference behavior. This is because, the model is operated in scramjet mode in the test while it is in ramjet mode in the calculation. On the other hand, for the case φ=0.25 in Fig. 8(b), although the pressure difference is still large, both the test and calculation indicate that the combustor is operating at ramjet mode, the overall behaviors of wall static pressure distribution from test and calculation are comparable.

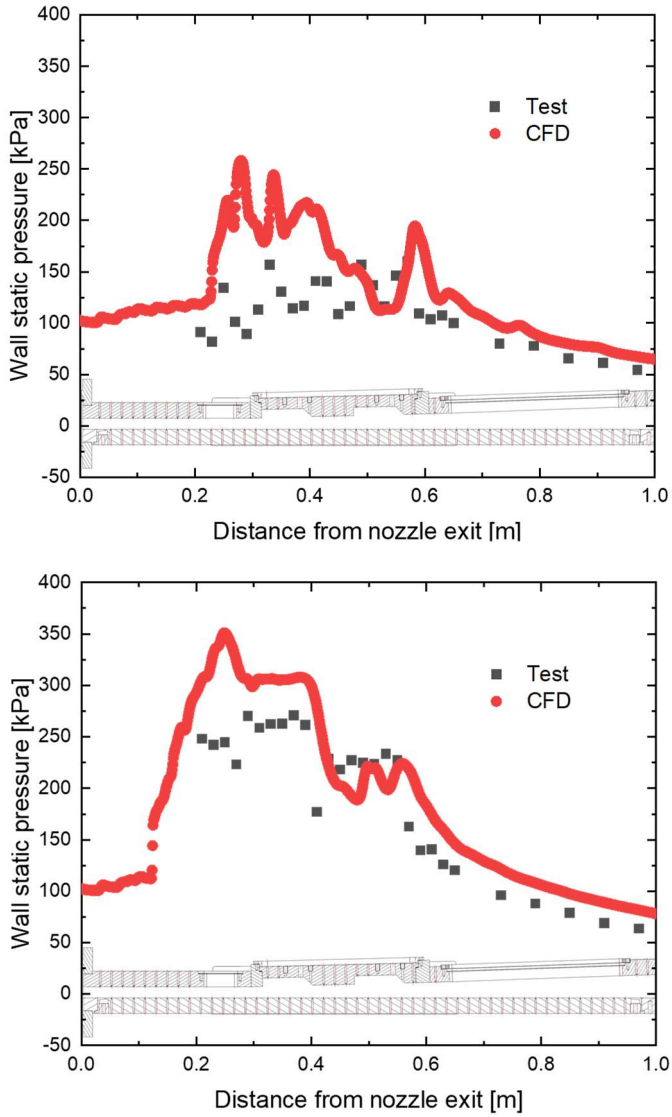

Fig. 8 Wall static pressure distribution by test measurement and calculation (top: (a) φ=0.12, (b) φ=0.25 case)

3.4. Fuel supply condition

Fig. 9 shows the fuel pressures and temperatures during the combustion tests. The values are measured at different points in the fuel flow path. For pressure as an example, one is at the fuel supply system and the other at the fuel injector. The pressure, based on the value are fuel injector, goes up to 1,000-2,100 kPa according to the fuel equivalence ratio.

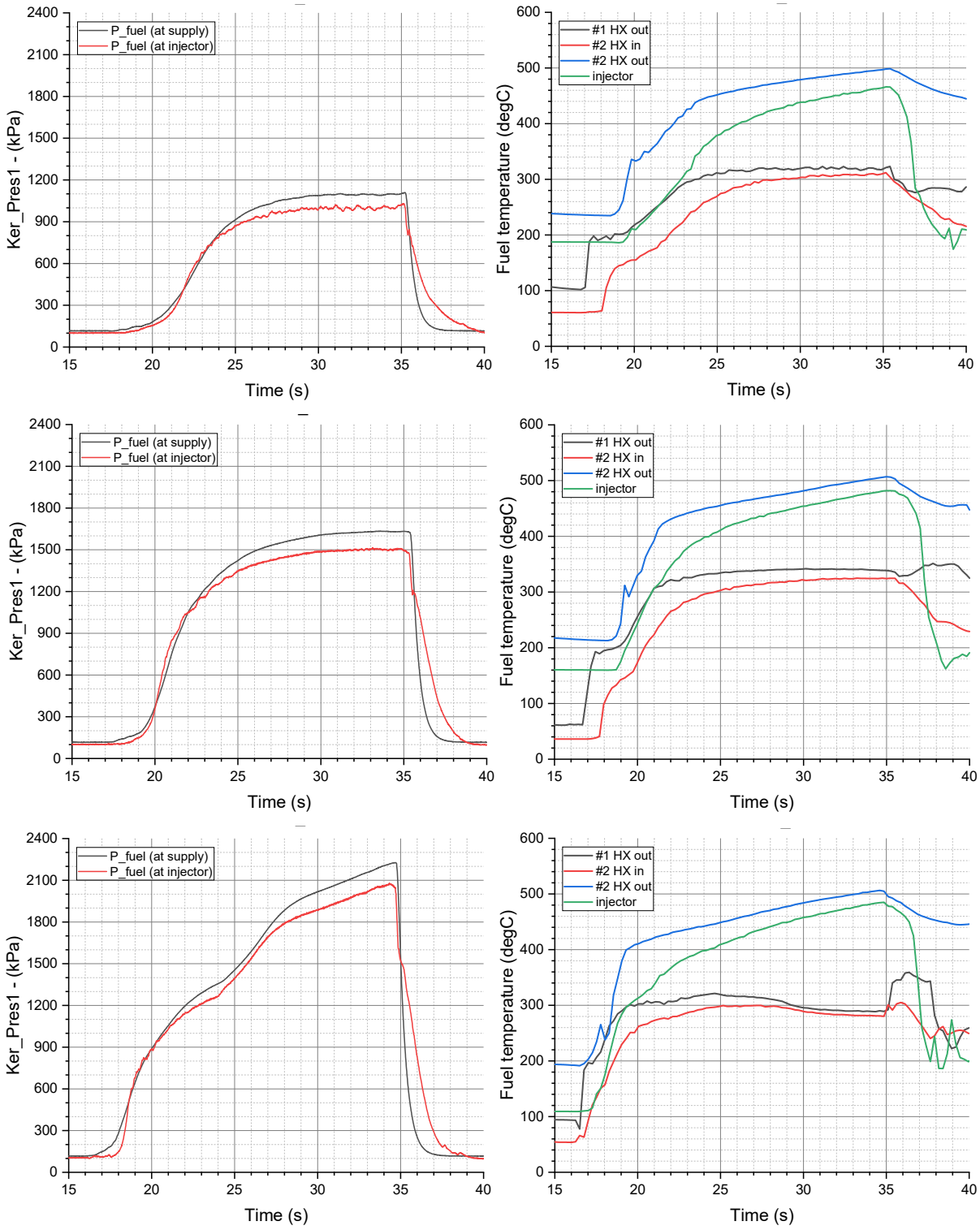

Fig. 9 Fuel pressure (left) and temperature (right) history (top: (a) φ=0.12, middle: (b) φ=0.19, bottom: (c) φ=0.25 case)

Between the two pressure measurement points, there are two regenerative heat exchangers in serial, one shut off valve and several fuel pipe segments. The difference between those two pressure values

is the pressure loss of the fuel path. And that pressure loss may be regarded as that of the two heat exchangers because those by the other components are small. One can find that the pressure loss is about 130 kPa at maximum, which is considered to be acceptable.

Regarding the fuel temperature history, it goes up to 500-503 °C right after the second heat exchanger, and 483-493 °C right before the fuel injector depending on the fuel equivalence ratio. The temperature decrease from #2 heat exchanger location to fuel injector location is due to the heat loss in the fuel pipe between those components One can note that the temperature difference, i.e. the heat loss, becomes smaller for larger fuel flow rate. The maximum temperature of 483-493 °C is higher than the fuel boiling temperature, even the critical temperature. Therefore, although the fuel is in subcritical state due to the low fuel pressure, it can be supercritical if the fuel pressure becomes higher by using smaller fuel injector.

Another thing to note is that the maximum fuel temperature is around 483-493 °C regardless of the fuel flow rate. In the authors' previous study, the maximum fuel temperature decreased when the fuel flow rate is increased. This was because the heat exchanging area is unchanged, and the increase in heat exchanged was not enough to heat up the increased fuel flow to the same temperature. Therefore, the result in the present research is attributed to the increased heat exchanging area. It may be expected that the maximum fuel temperature would not decrease with larger fuel flow than φ=0.25.

In the time period of t=25-30 s for all of the three test cases, the fuel temperature is relatively constant at the #1 heat exchanger out, while it increases continuously at the #2 heat exchanger out. The increase in this time duration is less than 5 °C by the former, while it is about 50 °C by the latter. This may be thought to be because the fuel phase change is occurring in the #1 heat exchanger. Fig. 10 is the property of the fuel used in this study, calculated using a surrogate model [6]. According to the figure, the fuel boiling temperature is between 560-580 K (287-307 °C) for the pressure of 1 MPa, and 620-640 K(347-367°C) for 2 MPa. These pressures and temperatures are similar to the fuel temperatures in the #1 heat exchanger. Therefore, one can assume that the fuel phase change is occurring in the #1 heat exchanger.

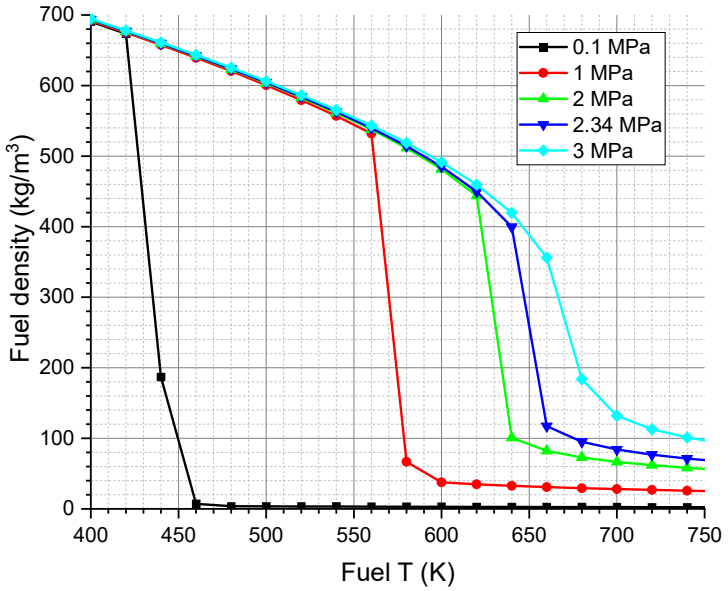

Fig. 10 Density of the fuel according to the pressure and temperature, calculated using surrogate model

4. Conclusion

Compared to the authors' results using models in previous researches, the results in the present study indicate that model transition is easier to realize using this model. By this mode transition, higher wall static pressure as well shorter flame length could be achieved. This may be attributed to several geometry changes from the previous models, but mainly to the smaller flow path height of this model. But on the other hand, half of the isolator length was occupied by the pre-combustion pressure rise

even at relatively low fuel equivalence ratio of 0.25. This indicates that the intake unstart may occur at low fuel equivalence ratio and the operational range in terms of fuel equivalence ratio will be reduced. This issue may be partly resolved by increasing the expansion angle of the combustor. The authors will try this design change in future researches.

References

1. Yang, I. et al.: Combustion performance according to the cavity flameholder location in a supersonic combustor. Journal of Korean Society for Propulsion Engineers V. 24 No. 5, 13-20 (2020)
2. Yang, I. et al.: Flame holding by regenerative cooling in a liquid-fueled supersonic combustor. Korean Society for Propulsion Engineers 2020 Fall Conference, KSPE 2020-2331 (2020)
3. Yang, I. et al.: Performance Consideration on the heat exchanger in a regenerative cooling supersonic combustor. Korean Society for Propulsion Engineers 2022 Spring Conference, KSPE 2022-1193 (2022)
4. Lee, K. et al.: Development of a scaled, ground test model of a turbine-based combined cycle engine, 11th Asia Joint Conference on Propulsion and Power, AJCPP2023-042 (2023)
5. Yang, I. et al.: Combustion test for a supersonic combustor using a direct-connected facility. Journal of Korean Society for Propulsion Engineers V. 22 No. 3, 1-7 (2018)
6. Lee, S. et al.: Prediction for heat transfer characteristics of supercritical kerosene using mixture surrogate. Korean Society for Propulsion Engineers 2017 Spring Conference, 294-296 (2017)